Korean J. of Chem. Eng., **10**(4), 211-219 (1993)

FLUID FLOW THROUGH 180° CURVED PIPE OF RADIANT TUBE

Heung Soo Park, Kil Won Cho, Yong Kuk Lee, Su Ki Park*, Young Cheol Kwon* and Moo Hwan Kim*

Energy Department, RIST, P.O. Box 135, Pohang 790-600, Korea
*Dept. of Mechanical Engineering, POSTECH, P.O. Box 125, Pohang 790-600, Korea
(Received 26 April 1993 • accepted 24 September 1993)

Abstract—The present study was carried out to investigate the flow characteristics through the curved section of a radiant tube which is used in the steel industry. The velocity profiles in the curved section were measured at a 1/2 scale water model apparatus by using 2D-LDV. The flow was also simulated numerically and a comparison was made with the experimental results. The flow characteristics in the curved section for various flow conditions of the burner was investigated. The secondary flow in the curved section and the flow stagnation phenomena at the end of the curved section were confirmed. It was found that the swirl velocity component imparted by the burner degrades the uniformity of flow and enlarges the stagnant region in the curved section. This flow pattern is supposed to cause non-uniform heat transfer and the local failure at the end of the curved section.

INTRODUCTION

A radiant tube (R/T) has been widely used as the equipment for indirect heating in the continuous annealing line of steel industry. The flow characteristics through the curved section in an R/T is known to be different from that through the straight section. As the flow enters a curved section, a centrifugal force acts outward from the center of curvature on the flow field. To maintain the momentum balance between the centrifugal force, w^2/R, and the pressure gradient, the secondary flow is supposed to be developed.

The flow through a curved pipe with a large curvature ratio ($\delta > 0.5$) usually arises in bio-fluid and R/T of continuous annealing line. In an R/T, hot combustion gas flows and a swirl velocity component is usually given by the burner to promote the combustion. The flow pattern through the curved section of the tube is very important to the temperature distribution of the tube and the life of tube material. The local failure of the R/T at the curved section, which often appears is thought to be related with the flow characteristics inside the tube, directly.

Theoretical studies on the flow through a curved pipe were first carried out by Dean [1]. He analyzed the secondary flow field as a deviation from Poiseuille flow by using the pertubation technique. Ito [2] summarized a lot of experimental researches. Agrawal et al. [3] measured the velocities of the developing flow of both axial and cross flow components by using LDV, and found an embedded vortex in addition to the secondary flow separation near the inner bend. Most of these investigations were devoted to the fully developed flow regimes or simple inlet conditions for small curvature ratio. For an R/T, it is needed to understand the flow characteristics through the curved section for various inlet flow conditions for optimal design of the burner.

The purpose of present study is to understand the flow characteristics in the curved section of an R/T for various flow conditions of the burner. An experimental apparatus was prepared using a glycerine-water solution as the simulant of the combustion gas. The flow characteristics were carefully studied by measuring the velocity profiles with 2D-LDV. A numerical simulation by using the PHOENICS computer code and a comparison with the experimental results were also carried out.

EXPERIMENTAL

1. Experimental apparatus

Fig. 1 shows the schematic diagram of the experimental set-up. The shape of the tube is same as the actual radiant tube in the continuous annealing line. The scale of the experimental apparatus is the half

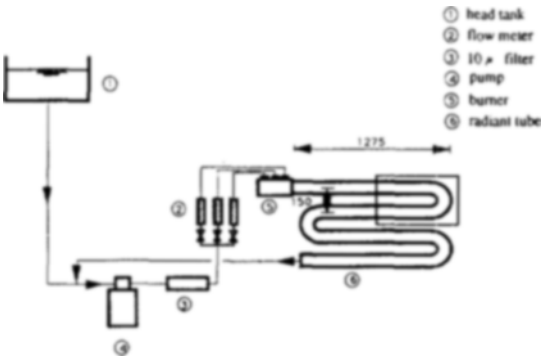

Fig. 1. Schematic diagram of experimental apparatus.

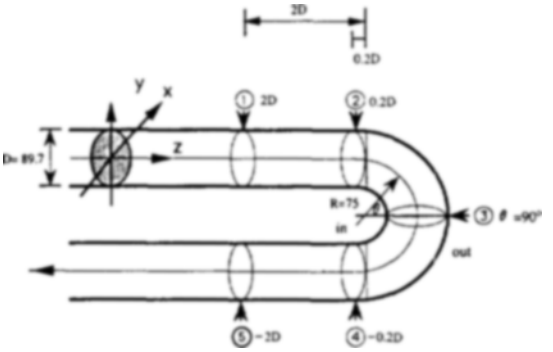

Fig. 2. Measuring positions in the curved pipe.

of actual equipment. The inner radius of the tube is 44.85 mm and the distance between the center lines of straight tubes is 150 mm. The burner is attached to the left end of the first straight tube. The fluid is delivered to the burner by the pump through a filter. The flow rate of the fluid entering the burner is controlled and measured by valves and float type flow meters. A 10 μm filter is installed between the pump and valves.

Fig. 2 indicates the curved section and the positions for measuring velocity profiles. The curvature ratio of the curved pipe was taken as $\delta = 44.85/75 = 0.598$. Mean velocities of axial and radial direction were measured at the upstream section [point (1)] and downstream section [point (5)], including the curved section [points (2), (3) and (4)].

Fig. 3 explains the detail of the model burner. The fluid is injected into the tube through the three nozzles, namely, fuel nozzle, primary and secondary air nozzles. Fuel nozzle is the innermost pipe. A 45° swirler is inserted in the primary air nozzle and imparting a swirl velocity component to fluid stream. The area ratio of nozzles was chosen as 1 : 4.8 : 6.59 to get the

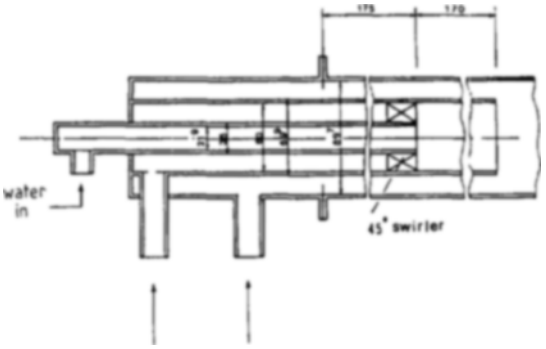

Fig. 3. Detail of the model burner.

Table 1. Flow rates at the burner nozzles

	Q_f m³/hr	Q_s m³/hr	Q_a m³/hr
Case 1	2.93	0	6.0
Case 2	2.93	6.0	0
Case 3	2.93	3.0	3.0

same condition as the actual burner.

A back scattering 2D-LDV system of two color four beam with 40 MHz optical frequency shift was used in the experiment. 2-Dimensional velocity components can be measured by means of two different modes of blue (488 nm) and green (514.5 nm) beam. y and z-directional velocity components were measured as shown in Fig. 2. The focal length of the beams are 310 mm and the size of the measuring volume is 0.079 mm×0.0079 mm×0.914 mm. A counter type signal processor was used for measuring the velocity from the Doppler signal.

2. Experimental method

A mixture of water and glycerine was used as the working fluid to minimize the effect of refraction of laser beams. The temperature of the fluid was 30℃ and the dynamic viscosity, ν, was measured as 4.352×10^{-6} m²/sec. The average axial velocity based on the total amount of the fluid entering the tube through the nozzles was calculated as 0.39 m/s and the Reynolds number and Dean number were 8083 and 6216, respectively. It belongs to turbulent flow regime.

Flow rates through the primary and the secondary nozzles, i.e., Q_s and Q_a, were varied under a fixed Q_f of 2.93 m³/hr. Table 1 indicates the inlet flow conditions at the burner nozzles.

For Case 1, there is no swirl velocity component. Strong swirl is imparted in condition of Case 2. Same amount of fluid with and without swirl velocity component is injected through the burner in condition of Case 3. Considering the fact that 30-50% of total com-

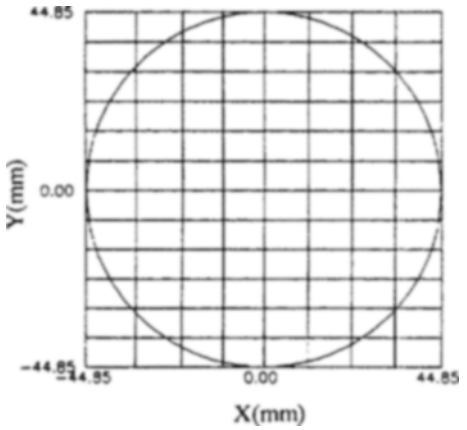

Fig. 4. Measuring grids on the plane of cross-section.
($\Delta X = 10.7$ mm, $\Delta Y = 7.5$ mm)

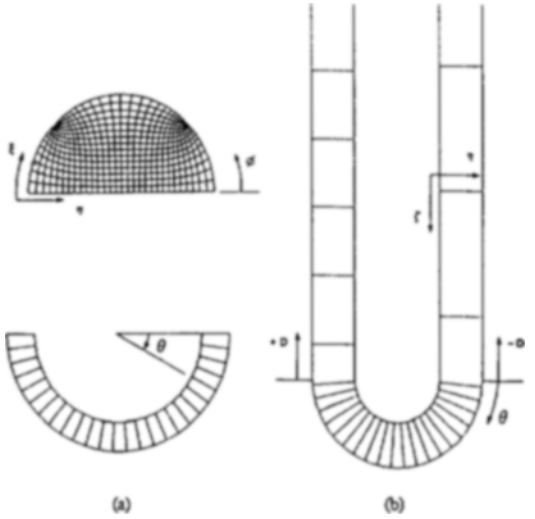

Fig. 5. Body-fitted grid system of curved pipe.
(a) Curved pipe (15×30×26), (b) Straight and curved pipe (15×30×39)

bustion air, generally, is injected through the primary nozzle in a 2-staged combustion type burner, Case 3 belongs to the practical flow conditions.

Fig. 4 illustrates the measuring grids on each plane of cross-section as shown in Fig. 2. The velocities were measured about from 70 points on each plane. The number of burst Doppler signal at each measuring point was set 500 and sampling time was taken to be 1 minute.

Reflective effects which cause incorrect measuring because of non-linear variation of fringe spacing and of the position and direction of the probe volume occur when LDV is used for measuring the fluid velocity inside a circular tube. Moreover, proper imaging of the beam intersection on the pin hole of a photo detector as well as the collection of Doppler signals can be a severe problem. To overcome these problems, the tube is placed in a rectangular optical box filled with the same fluid as the working fluid for compensating some of the refractive effects.

Applying the compensating method of refraction error of beam by Gardavask [4], deviation of the location of measuring volume is proved to be accurate within 5% of measuring grid interval and that of fringe spacing is within 1%, in the range of 90% of tube inside diameter.

NUMERICAL METHOD

The flow phenomena in a curved pipe is very complicated. PHOENICS computer code is used to solve simultaneously the flow field for both the curved and the straight sections of the R/T with body-fitted coordinate system. The computation is carried out only for the inlet condition of without swirl at the burner. It is thought that the domain of computation can be considered as symmetrical half-section of the tube since the flow is symmetrical.

Fig. 5 shows the grid system generated by three dimensional elliptic grid generation technique for the calculation. The geometry of the pipe is same as that of experiment and $15(\xi)\times30(\eta)$ grids are used on the plane of cross-section. The curved section has 26 grids along the flow direction and the upstream and downstream straight sections has 4 and 9 grids, respectively.

The turbulent calculation at the same inlet condition with the Case 1 of Table 1 was carried out. In the present study the standard k-ε turbulence model was adopted. The turbulent viscosity μ_t is expressed as

$$\mu_t = C_\mu \rho k^2/\varepsilon$$

Where C_μ is a constant of which value is 0.09. The governing equations for k and ε have the following source terms;

Turbulence energy k:

$$\mu_t\left(\frac{\partial u_i}{\partial x_k}+\frac{\partial u_k}{\partial x_i}\right)\frac{\partial u_i}{\partial x_k}-\rho\varepsilon$$

Dissipation rate ε:

$$C_1\mu_t\frac{\varepsilon}{k}\left(\frac{\partial u_i}{\partial x_k}+\frac{\partial u_k}{\partial x_i}\right)\frac{\partial u_i}{\partial x_k}-C_2\rho\frac{\varepsilon}{k}$$

The empirical constants of the turbulent model have been chosen as the following commonly used values.

$C_1 = 1.44$, $C_2 = 1.92$

The values of turbulent Prandtl numbers for the diffusive transport of k and ε have been chosen as 1.0 and 1.3, respectively. The wall function method was used for accounting for the near wall region.

The elliptic form of governing equations necessitates boundary conditions. Because no swirl velocity component is imparted at the burner, the only axial velocity, which is measured, is given at the inlet of calculation domain. At the outlet of the tube, it is assumed that the flow is fully developed. The symmetry conditions are imposed on the plane of symmetry.

The boundary conditions are as follows;

inlet :

$u = 0$

$v = 0$

w = average of measured value by experiment

outlet :

$$\frac{\partial w}{\partial \zeta} = 0,\ u = v = 0$$

plane of symmetry :

$$u = \frac{\partial v}{\partial \xi} = \frac{\partial w}{\partial \xi} = 0$$

wall :

no slip

RESULTS AND DISCUSSION

1. Comparison of experimental and computational results

A comparison between the numerical and experimental results was carried out at the inlet condition of no swirl velocity component (Case 1). Fig. 6 compares the mean axial velocity contours. The contours appear at every 0.05 m/sec in the figure. In the first straight pipe, between the burner and the curved section, there exists a potential core in the flow. The magnitude of the axial velocity is nearly the same as the average velocity. The flow seems to be under developing. As the fluid reaches the curved section (position 2), the location of the maximum axial velocity shifts down by the fluid particles moving toward the lower wall of the tube by the effect of downstream. The experimental and computational results show same trend and this flow pattern is generally found in the flow of curved pipe [5].

As the fluid reaches the center of curved section (position 3), two peaks of axial velocity appear symmetrically and a steep gradiant of axial velocity is seen near the inner wall. The maximum axial velocity is 1.4 times higher than the average velocity. The peaks seem to be occurred by the development of the secondary flow which moves the fluid particles outward in the center region and inward along the both side walls on the plane of cross-section. The peaks are more clear in the experimental result. The center of the secondary flow appears near the inner wall. The development of the secondary flow in the curved section seems to be retarded in the computation. The computational results shows the location of the maximum axial velocity near inner wall. This is also by the delay

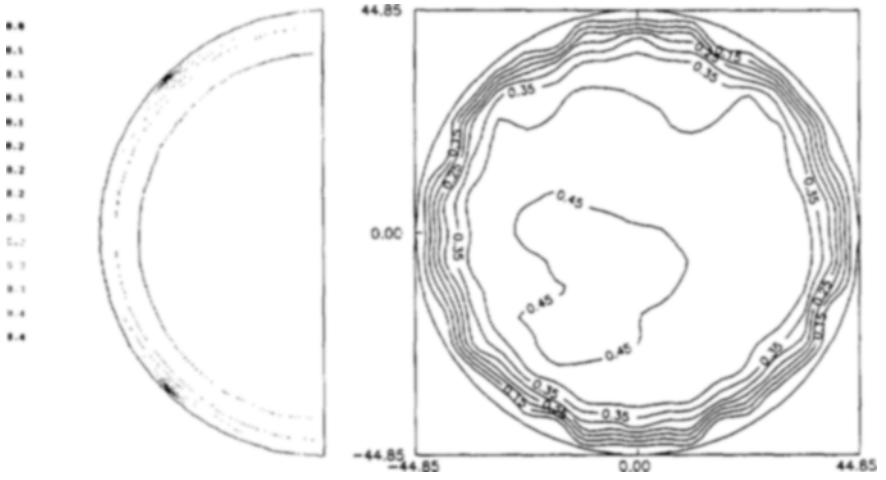

Fig. 6. Comparison of axial velocity contours on the plane of cross-section in the case of no swirl inlet condition.
(left : calculation, right : measurement)

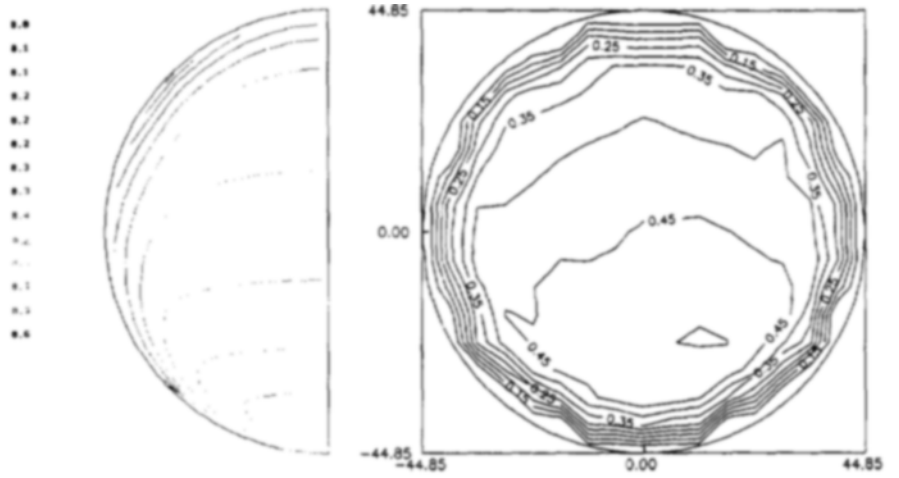

(b) - 0.2D

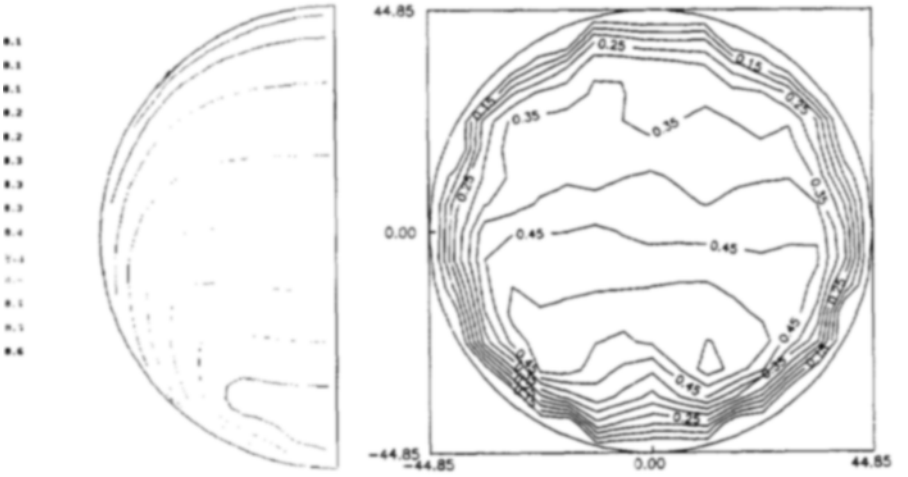

(c) $\theta = 90°$

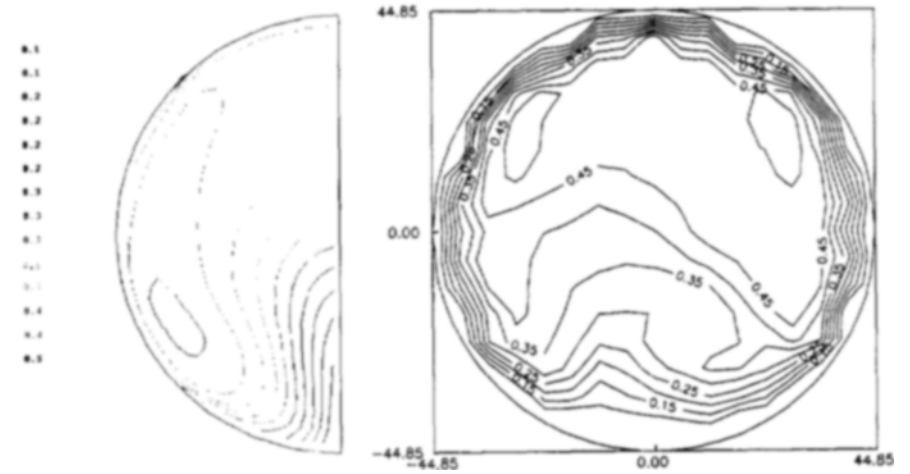

(d) 0.2D

Fig. 6. continued.

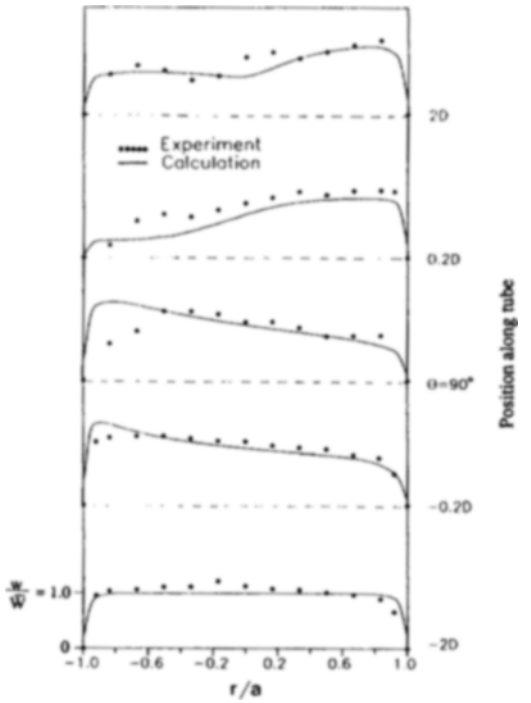

Fig. 7. Comparison of axial velocity distributions on the plane of symmetry in the case of no swirl inlet condition.

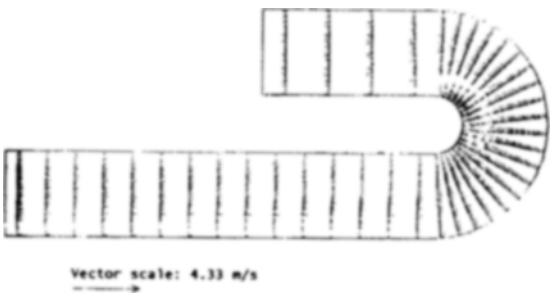

Fig. 8. Calculated velocity vector distribution on the plane of symmetry in the case of no swirl inlet condition.

of the development of secondary flow in the curved section, which is supposed to be occurred by the difference of downstream between the computation and experiment.

At the outlet of the curved pipe (position 4), there exists a large inviscid region near the inner wall and the peaks of maximum axial velocity departs each other. In the experiment, the location of these peaks is found near the outer wall. The discrepancy of the location of the velocity peaks between the experiment and computation is caused by the effect of upstream.

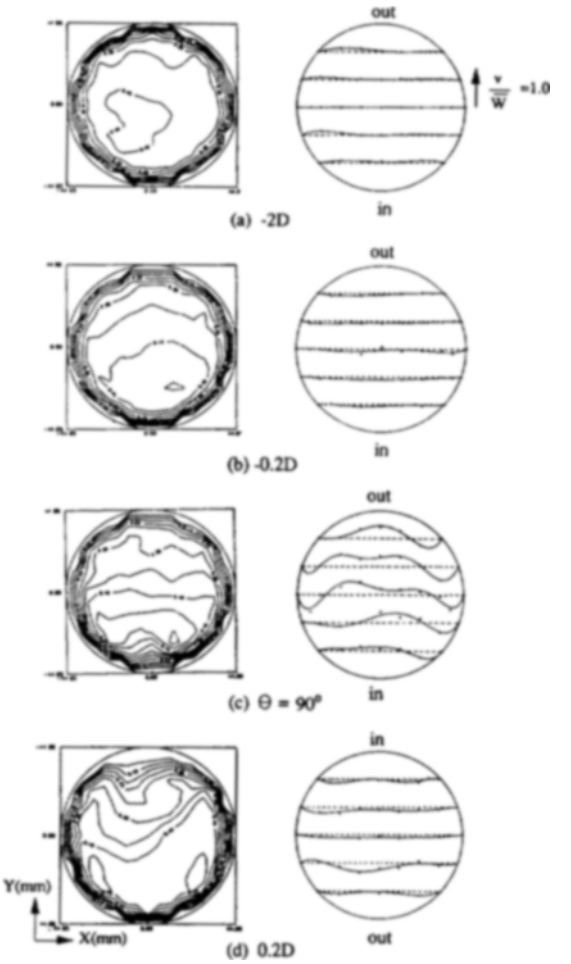

Fig. 9. Axial velocity contours and secondary velocity profiles on the plane of cross-section (case 1).

Fig. 7 compares the axial velocity distributions on the plane of symmetry. The computational results show good agreement with the experiment except inner wall region of the curved section. The measured value is lower than that by computation because of the separation of fluid particles from the inner wall by the secondary flow. The deviation of axial velocity on the plane of cross-section is most severe at the outlet of the curved pipe. The axial momentum is recovered as the fluid passes out the curved section.

As pointed out by earier researchers [6], it is considered that the turbulence modeling is one of the factors which cause the discrepancy between computation and experiment, especially in the curved section.

Fig. 8 shows the axial velocity vector distribution

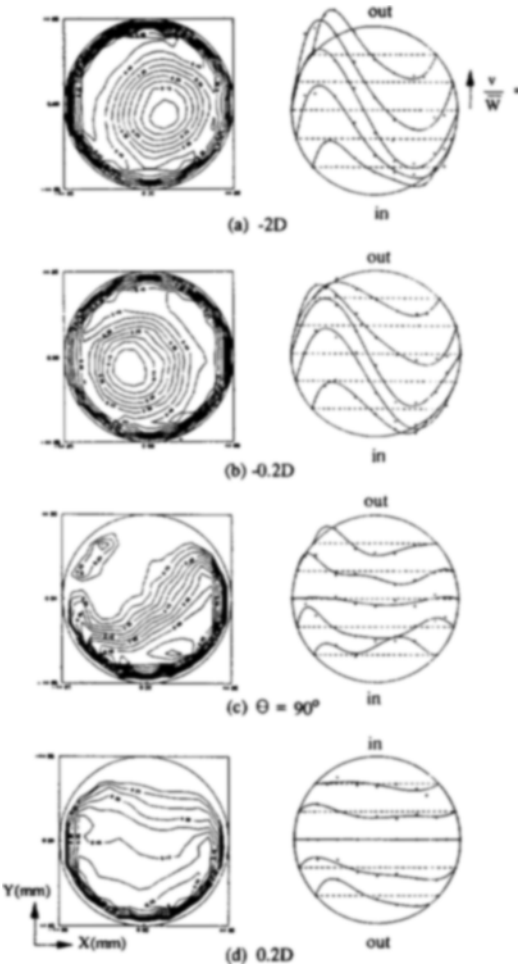

Fig. 10. Axial velocity contours and secondary velocity profiles on the plane of cross-section (case 2).

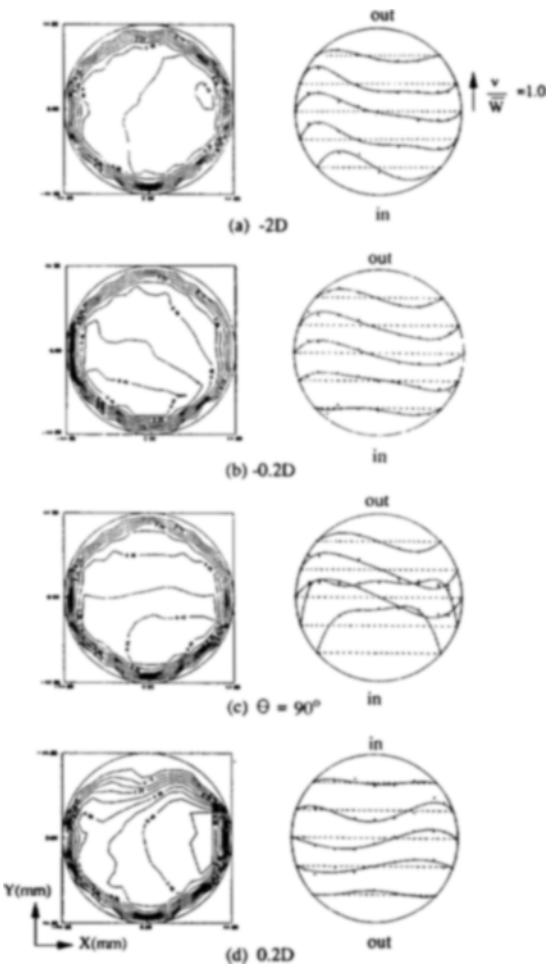

Fig. 11. Axial velocity contours and secondary velocity profiles on the plane of cross-section (case 3).

obtained by computation. It was found both in the experimental and computational results that the location of peak axial velocity and the center of the secondary flow appears near the inner wall in the curved section. This is interesting phenomenon compared with the flow patterns with a small curvature ratio and an intermediate range of Dean number. The flow pattern in the curved pipe is affected by the Dean number and the curvature ratio. It is generally known that the center of the secondary flow appears in the center region on the plane of cross-section when the curvature ratio is small [7]. Sumida [8] discovered that the center of the secondary flow moves toward the inner wall and the region of weak viscosity effect forms near the outer wall as the curvature ratio increases.

2. Flow patterns in curved section

The effect of flow conditions at the burner on the flow patterns in the curved section is investigated, based on the experimental results as shown in Fig. 9-12.

In case of no swirl inlet condition (Fig. 9), the secondary flow in the curved section arises as can be seen in ordinary curved pipes, but the centers appear near inner wall. This secondary flow diminishes as the fluid passes out the curved section by interchange of momentum. At the outlet of the curved section, a stagnant region appears near the inner wall.

Fig. 10 shows the flow patterns when a strong swirl velocity component is imparted from the primary nozzle of the burner (Case 2). The magnitude of swirl velocity is 1.7 times higher than that of the average axial velocity. By this swirling flow, the maximum val-

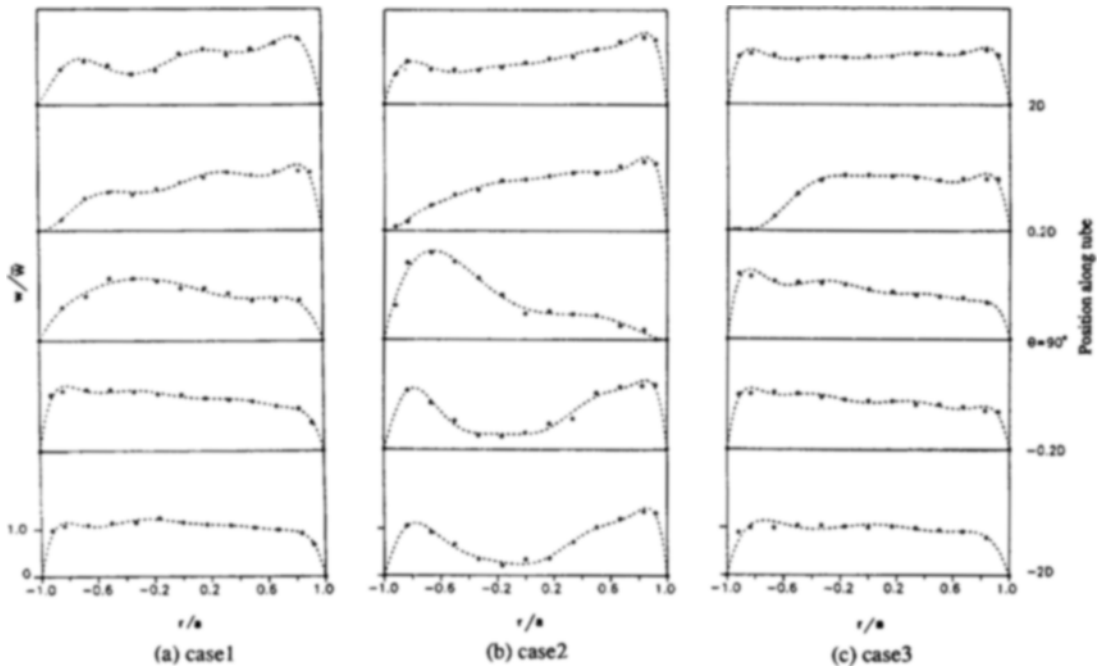

Fig. 12. Comparison of axial velocity distributions on the plane of symmetry.

ue of axial velocity appears circumferentially near the tube wall and the magnitude is about 1.4 times of the average axial valocity The shift down of the location of the maximum axial velocity at the inlet of the curved section, as shown in Fig. 6, is not found. By the precessing vortex which can be seen in the swirling flow in a circular tube, it is supposed that the center of the swirling flow moves spirally as the fluid passes through the first straight tube [9].

The secondary flow and two peaks of axial velocity are found as the case of no swirl inlet condition but the direction of the secondary flow is reversed. The fluid particles move outward along the both side walls and move inward along the axis of symmetry. Since the fluid enters with swirl velocity component, a centrifugal force acts on the fluid particles to radial direction. At the same time, another centrifugal force caused by the curvature of tube lifts the fluid particles to the y-direction on the plane of cross-section. The combination of these two kinds of forces makes the fluid particles move outward along the both side walls. The force which acts outward on the fluid particles of right half zone diminishes by the clockwise flow. The fluid particles moving outward along the left wall is, however, accelerated. This causes the non-symmetric secondary flow pattern on the plane of cross-section. The fluid particles moving inward at the center zone make the gradient of axial velocity steeper and form a larger inviscid region in outer half zone on the plane of cross-section. The maximum axial velocity is about three times higher than that in case of no swirl inlet condition. The flow is accomplished through the half cross-sectional area, which is supposed to cause the non-uniform heating of the tube in actual equipments. At the outlet of the curved pipe, the secondary flow diminishes in spite of strong swirl at the inlet of the curved section.

Fig. 11 is for the case that the same amount of fluid is injected through the primary and secondary nozzles. The flow pattern in the first straight pipe is similar to that of the case of strong swirl, but the intensity of swirling flow is weak. At the center of the curved section, it is found that the secondary flow on the plane of cross-section is bisected. Near the inner wall at which the magnitude of centrifugal force by the curvature is comparatively higher than that near the outer wall, the swirling flow disappears and the fluid particles move outward. The swirling flow remains in the outer region.

Fig. 12 compares the axial velocity distributions on the plane of symmetry for above three cases of inlet conditions. It is found that the swirl velocity component imparted at the burner enhances the deviation of velocity distribution and enlarges the stagnant region at the outlet of the curved section. It is also noted that the axial momentum is recovered at the

downstream of the curved section for all cases. The deviation of axial velocity on the plane of cross-section is most severe in case of strong swirl inlet condition. But the stagnant region near the inner wall at the outlet, which is supposed to cause the hot spot and non-uniform heat transfer, is severe in the case of medium swirling condition. In an R/T, it is concluded that the swirling flow given by the burner degrades the uniformity of the flow in the curved section and this can make non-uniform heat transfer which leads to the local failure of tube.

CONCLUSION

The flow characteristics in the curved section of a radiant tube was investigated by numerical analysis and experiment for various inlet conditions at the burner.

It was found that the center of secondary flow in the curved pipe appears near the inner wall by both the computation and experiment in the radiant tube geometry. The swirling flow given by the burner acts strong influence on the secondary flow patterns and causes non-uniform flow and stagnant region at the outlet of the curved pipe. It is also found that the swirling momentum diminishes as the fluid passes out the curved section. It is recommended that the swirling velocity component should be excluded for uniform heating of the tube in actual equipment.

NOMENCLATURE

a : inner radius of radiant tube
D : inner diameter of radiant tube
Q_F : flow rate through fuel nozzle
Q_S : flow rate through primary air nozzle
Q_0 : flow rate through secondary air nozzle
R : radius of curvature
u, v, w : mean velocities
x, y, z : coordinate system
De : Dean number $=\delta^{1/2}(2\ au/v)$
δ : curvature ratio $=a/R$
v : viscosity

REFERENCES

1. Dean, W. R.: *Philos. Mg.*, **5**, 673 (1928).
2. Ito, H.: *Trans. ASME, J. Basic Engng.*, 123 (1982).
3. Agrawal, Y., Talbolt, L. and Gong, K.: *J. Fluid Mech.*, **85**, 497 (1978).
4. Gardavsk, J., Hrbek, J., Chara, Z. and Severa, U.: Dantec infor. No. 08 Nov. (1989).
5. Olson, D. E. and Snyder, B. J.: *J. Fluid Mech.*, **150**, 139 (1985).
6. Patankar, S. V., Pratap, V. S. and Spalding, D. B.: *J. Fluid Mech.*, **67**, part 3, 592 (1975).
7. Tanishita, K., Suzuki, J., Ohishi, N. and Naruse, T.: *T. JSME(B)*, **57**, 898 (1991).
8. Sumida, M., Sudou, K. and Yuhara, A.: *T. JSME(B)*, **54**, 498, 297 (1988).
9. Syred, N. and Beer, J. M.: *Combustion and Flame*, **23**, 191 (1974).